Chemistry and Physics of Lipids xxx (xxxx) xxx–xxx

Contents lists available at ScienceDirect

Chemistry and Physics of Lipids

journal homepage: www.elsevier.com/locate/chemphyslip

IR spectroscopy analysis of pancreatic lipase-related protein 2 interaction with phospholipids: 3. Monitoring DPPC lipolysis in mixed micelles

Eduardo Mateos-Diaz[a], Priscila Sutto-Ortiz[a,b], Moulay Sahaka[a], Jorge A. Rodriguez[b], Frédéric Carrière[a,*]

[a] Aix-Marseille Université, CNRS, UMR7282 Enzymologie Interfaciale et Physiologie de la Lipolyse, Marseille, France
[b] Biotecnología Industrial, Centro de Investigación y Asistencia en Tecnología y Diseño del Estado de Jalisco A.C. (CIATEJ), Zapopan, Jalisco, México

ARTICLE INFO

Keywords:
Enzyme
FTIR spectroscopy
Lipids
Lipid digestion
Lipolysis
Phospholipase

ABSTRACT

Usual methods for the continuous assay of lipolytic enzyme activities are mainly based on the titration of free fatty acids, surface pressure monitoring or spectrophotometry using substrates labeled with specific probes. These approaches only give a partial information on the chemistry of the lipolysis reaction and additional end-point analyses are often required to quantify both residual substrate and lipolysis products. We used transmission infrared (IR) spectroscopy to monitor simultaneously the hydrolysis of phospholipids by guinea pig pancreatic lipase-related protein 2 (GPLRP2) and the release of lipolysis products. The substrate (DPPC, 1,2-Dipalmitoyl phosphatidylcholine) was mixed with sodium taurodeoxycholate (NaTDC) to form mixed micelles in D_2O buffer at pD 6 and 8. After hydrogen/deuterium exchange, DPPC hydrolysis by GPLRP2 (100 nM) was monitored at 35 °C in a liquid cell by recording IR spectra and time-course variations in the CO stretching region. These changes were correlated to variations in the concentrations of DPPC, lysophospholipids (lysoPC) and palmitic acid (Pam) using calibration curves established with these compounds individually mixed with NaTDC. We were thus able to quantify each compound and its time-course variations during the phospholipolysis reaction and to estimate the enzyme activity. To validate the IR analysis, variations in residual DPPC, lysoPC and Pam were also quantified by thin-layer chromatography coupled to densitometry and similar hydrolysis profiles were obtained using both methods. IR spectroscopy can therefore be used to monitor the enzymatic hydrolysis of phospholipids and obtain simultaneously chemical and physicochemical information on substrate and all reaction products (H-bonding, hydration, acyl chain mobility).

1. Introduction

Many methods and techniques have been used for the detection and assay of lipolytic enzymes (Beisson et al., 2000; Mateos-Diaz et al., 2012). Some of these methods rely on the release of hydrolysis products, mainly the fatty acids, or the consumption of the substrate and can be used for the continuous assay of enzyme activities and for monitoring enzyme kinetics. Among them, titrimetry of free fatty acids (FFA) released during the lipolysis reaction is a common method that has been applied to the assay of lipase activity on various triglyceride emulsions, as well as phospholipase and galactolipase activities on micellar substrates (Amara et al., 2009; Brockman, 1981; de Haas et al., 1968; Dennis, 1973; Desnuelle et al., 1955; Gargouri et al., 1986). Other common methods are based on spectrophotometry using fluorescent (parinaric acid (Beisson et al., 1999)) or UV-absorbing (α-eleostearic acid (El Alaoui et al., 2016; Mendoza et al., 2012; Pencreac'h et al., 2002; Serveau-Avesque et al., 2013), punicic acid (Ulker et al., 2016)) fatty acids present in natural or synthetic substrates, fluorescent probes grafted onto the lipid substrate such as boron-dipyrromethene (BODIPY® (Feng et al., 2002; Heinze and Roos, 2013)) or pyrene (Negre et al., 1988), pH indicators sensitive to FFA release (Camacho-Ruiz Mde et al., 2015; Mateos-Diaz et al., 2012; Sutto-Ortiz et al., 2017) or simply color developing reagent reacting with FFA (Kwon and Rhee, 1986). Because these assays do not allow monitoring the supramolecular assembly of the substrate and changes occurring upon lipolysis, assays based on interfacial tensiometry (monomolecular films (Ransac et al., 1991; Verger and de Haas, 1973, 1976), oil-drop tensiometer (Labourdenne et al., 1994; Nury et al., 1987)) have been developed, but they are limited to the kinetic characterization of highly purified enzymes and are impaired by the presence of surfactants.

Abbreviations: ATR, attenuated total reflection; DPPC, 1,2-di-palmitoyl phosphatidylcholine; FTIR, Fourier transform infrared spectroscopy; FWMH, full width at mean height; GPLRP2, guinea pig pancreatic lipase-related protein 2; NaTDC, sodium taurodeoxycholate; Pam, palmitic acid; PLRP2, pancreatic lipase-related protein 2; TLC, thin layer chromatography

* Corresponding author at: CNRS, UMR7282 EIPL, 31 chemin Joseph Aiguier, 13402 Marseille cedex 20, France.
E-mail address: carriere@imm.cnrs.fr (F. Carrière).

https://doi.org/10.1016/j.chemphyslip.2017.11.009
Received 15 August 2017; Received in revised form 4 November 2017; Accepted 8 November 2017

Chromatographic techniques (GC, HPLC, TLC) coupled with various detection methods usually provide a more complete description of the lipolysis reaction with the parallel analysis of residual substrate and hydrolysis products (Ackman et al., 1990; Cavalier et al., 2009; Tarvainen et al., 2011). Although these methods often allow a complete and quantitative analysis of lipolysis products, they require an extraction step prior to the analysis itself and cannot be used for a direct and continuous assay of the reaction kinetics. Moreover, the extraction step has to be validated with reference standards in order to ensure the full recovery of lipolysis products and eventually apply correction factors if the recovery is not complete (Cavalier et al., 2009). The various assays described above have often to be combined for a better understanding of lipolytic enzyme activity on complex lipid substrates. This is a time-consuming and laborious approach and there is a quest for single methods giving access to overall enzyme activity, quantification of reaction products and physico-chemical information on lipid assemblies at the same time. Here we explore the use of Infrared (IR) spectroscopy for studying enzyme-catalyzed lipolysis reactions.

IR spectroscopy is a versatile technique based on the vibrational state of atomic bonds and thus it is a suitable technique for the study of chemical changes and physicochemical properties simultaneously (Lewis and McElhaney, 2013; Mendelsohn and Moore, 1998; Snabe and Petersen, 2002). There are already some publications reporting the use of transmission IR spectroscopy to investigate lipase-catalyzed hydrolysis of TAGs in reverse micelles and organic solvent (O'connor and Cleverly, 1994 Walde and Luisi, 1989). In other studies, changes in the secondary structure of phospholipase A_2 (PLA_2) upon interaction with lipids and during hydrolysis were investigated using by both attenuated total reflection (ATR) and transmission IR spectroscopy (Kennedy et al., 1990; Tatulian, 2001; Tatulian et al., 1997), but lipid hydrolysis was not directly studied by IR spectroscopy. Snabe et al. proposed an ATR-IR spectroscopy method to monitor the hydrolytic activity of *Fusarium solani* cutinase on surface-coated film of triglyceride (Snabe and Petersen, 2002). The use of supported lipid films on the ATR crystals was however limited by the possible film disruption and/or desorption of both substrate and lipolysis products from the surface in the course of the reaction and in the presence of surfactants (Snabe and Petersen, 2002). Much of the spectral information gained in these previous studies was not exploited, probably due to the molecular complexity and dynamics of the systems investigated. To limit this complexity, we previously investigated by IR spectroscopy the first step of the lipolysis reaction, *i.e.* the interfacial recognition of supersubstrates, using an inactive variant of guinea pig pancreatic lipase-related protein 2 (GPLRP2 S152G; see the accompanying paper by Mateos-Diaz et al. (Mateos-Diaz et al., 2017)) and we were able to identify specific changes in the IR spectrum of DPPC reflecting the interaction of the GPLRP2 variant with DPPC-bile salt micelles.

The present work was performed using the same DPPC-bile salt micelles and the active GPLRP2 enzyme. We propose a new and relatively simple method to measure phospholipase activity on phospholipid-surfactant mixed micelles using transmission IR spectroscopy in D_2O. The time-course hydrolysis of DPPC has been monitored by recording IR-spectra of the entire reaction mixture as a function of time. Kinetics of the reaction, lipolysis product quantification and some changes in the physicochemical properties of the reaction mixture were followed using characteristic regions of the IR spectrum: hydrophobic acyl chain CH stretching, interfacial CO and COO^- stretching bands and the PO and ROPOR headgroup vibrations.

2. Materials and methods

2.1. Reagents

1,2-dipalmitoyl-*sn-glycero*-3-phosphocholine (DPPC) and 1-palmitoyl-2-hydroxy-*sn-glycero*-3-phosphocholine (lysoPC), both > 99% purity, were obtained from Echelon Biosciences Inc. Palmitic acid (Pam), sodium taurodeoxycholate (NaTDC), 2-(N-morpholino)-ethanesulfonic acid (MES), 2-Amino-2-(hydroxymethyl)propane-1,3-diol (Tris), 4-(2-hydroxyethyl)-1-piperazineethanesulfonic acid (HEPES), deuterium oxide (D_2O) 99.9%, benzamidine and dithiothreitol (DTT) were purchased from Sigma-Aldrich. Heptane, ethyl ether, acetic acid, chloroform and methanol were all HPLC grade from Carlo Erba. Calcium chloride ($CaCl_2$) and sodium chloride (NaCl) were obtained from Euromedex.

2.2. Production and purification of recombinant GPLRP2

Recombinant wild-type GPLRP2 was produced and purified as previously described in the accompanying article (Mateos-Diaz et al., 2017).

2.3. Preparation of DPPC-NaTDC mixed micelles

Monodispersed mixed micelles of DPPC and NaTDC were prepared as described in the accompanying article (Mateos-Diaz et al., 2017) using either 100 mM MES or 100 mM Tris buffers for experiments at pH 6 or 8, respectively. Both buffer solutions also contained 150 mM NaCl, 5 mM $CaCl_2$ and 50 mM NaTDC. The final DPPC concentration was 68 mM (5%, w/v) and the DPPC to NaTDC molar ratio was 1.36. For IR studies, the micelles were prepared using D_2O and 100 mM HEPES buffer was used instead of Tris in all the experiments at pD 8. All the steps involving D_2O manipulation were performed under argon atmosphere to avoid hydrogen/deuterium back-exchange and all the buffer solutions were prepared considering that pD = pH + 0.4.

2.4. Hydrolysis of DPPC-NaTDC mixed micelles by GPLRP2

DPPC hydrolysis reactions were carried out using 5 pmoles of recombinant GPLRP2 added to 50 µL of the DPPC-NaTDC mixed micelles (100 nM final enzyme concentration) at pD/pH 6 or 8 and 35 °C. This reaction volume was adapted for monitoring DPPC hydrolysis by transmission IR spectroscopy for 120 min. Similar reaction volumes were used for studying DPPC hydrolysis by thin-layer chromatography (TLC), but for each conditions of pH, six separate reactions were prepared and incubated for 0 (control), 20, 40, 60, 80 or 120 min before stopping the reaction by addition of the solvent for lipid extraction. This procedure allowed the time-course analysis of lipolysis products by TLC as described in section 2.6.

2.5. Analysis of DPPC hydrolysis by transmission infrared spectroscopy

Fifty µL of the DPPC hydrolysis reaction were placed and squeezed between the two CaF_2 transmission crystals with a 50 µm spacer of polytetratfluoroethylenelene (Teflon). IR-spectra were then recorded each 5 min during 2 h at 35 °C using a JASCO™ FT/IR-6100 Fourier transform infrared spectrometer. All the spectral parameters were the same used in the accompanying study (Mateos-Diaz et al., 2017). The analysis of IR spectra was focused mainly on the carbonyl (CO) and carboxylate (COO^-) stretching bands. For the deconvolution of the CO band spectra (when applies), an initial full width at mean height (FWMH) estimation of 24 cm^{-1} was used (Lefevre and Subirade, 2000).

2.6. Extraction of lipolysis products and TLC analysis

Each 50-µL hydrolysis reaction dedicated to TLC analysis was stopped by adding 50 µL of 1 N HCl solution and then diluted with water to a final volume of 250 µL. For lipid extraction, 500 µL of chloroform/methanol (2/1) (v/v) were added. After vigorous shaking and phase separation, the lower organic phase was collected using a Pasteur pipette and transferred to a 2 mL tube. It was dried with anhydrous $MgSO_4$, which was then removed by centrifugation for 1 min at 1,000*g*. The lipid extracts in chloroform/methanol were kept at −20 °C

until the TLC analysis was performed.

The presence of residual DPPC and released lipolysis products in the different lipid extracts was assessed by TLC after spotting 25 µL of each lipid extract on a 10 × 20 cm glass plates coated with 0.2 mm silica gel 60 (Merck) using a Linomat IV sample spotter (Camag, Muttenz, Switzerland). Lipolysis product separation was achieved by a double migration using first chloroform/methanol/water (65/35/5 v/v/v) and second, heptane/ethyl ether/formic acid (55/45/1 v/v/v). After separation, the plate was dried and lipolysis products were revealed by charring the plate after dipping it with a mixture (50:50) (v/v) of saturated solution copper acetate in water and 85.5% phosphoric acid.

The quantitative analysis of DPPC, lysoPC and Pam was performed by densitometry at 500 nm with a CAMAG TLC scanner 3 (Camag, Muttenz, Switzerland), using pure DPPC, lysoPC and Pam at different concentrations as reference standards.

2.7. GPLRP2 activity measurements using the pHstat technique

Phospholipase activity of GPLRP2 was measured by automated titration of fatty acids released from stirred DPPC (16.3 mM) dispersions, using 0.1N NaOH and a TTT80 Radiometer™ pH-Stat (Copenhagen). Each assay was performed in a thermostated vessel (37 °C) containing 1 mM buffer (MES or Tris for pH 6 or 8, respectively) with 150 mM of NaCl, 5 mM of $CaCl_2$ and 12.5 mM of NaTDC (DPPC-to-NaTDC molar ratio of 1.3). Back-titration at pH 9 was performed for assays at pH 6 to avoid underestimating enzymatic activity due to partial ionization of palmitic acid. One unit of enzymatic activity (U) corresponds to 1 µmol of free fatty acid released per min.

3. Results and discussion

3.1. Overall changes observed in the IR spectrum upon lipolysis

The interpretation of the changes at the different regions of the IR spectra reveals information about the fluctuations occurring in the vibrations of specific chemical bonds (Lewis and McElhaney, 2013; Mendelsohn and Moore, 1998). Typically, peak-shifts, broadening or narrowing, and differences in relative intensities may be related to physicochemical changes occurring in a sample. In the case of DPPC hydrolysis by GPLRP2, palmitic acid (Pam) and lysoPC molecules are released, producing a rather complex lipid mixture with dynamic physicochemical properties and multiple spectral features. Fig. 1A shows the IR-spectra of a mixed DPPC-NaTDC micellar dispersion recorded before and after 120 min of hydrolysis by GPLRP2 at pD8. The nature and intensity of the spectral changes caused by the hydrolysis of DPPC vary considerably depending on the spectral region, but the main vibrations of interest are the CH stretching vibrations of the hydrophobic acyl chains (asymmetric $\nu_{as}CH_2$ and symmetric ν_sCH_2 at 2923 and 2854 cm^{-1}), the carbonyl stretching vibration (νCO at 1735 cm^{-1}), the carboxylate stretching vibration (νCOO^- at ≈1500 cm^{-1}), the CH_2 scissoring vibration ($\nu_{sci}CH_2$ at ≈1470 cm^{-1}) and the head-group PO stretching vibrations (symmetric ν_sPO and ν_sROPOR' at 1089 and 1060 cm^{-1}). Fig. 1B, shows in more detail the CH stretching region (3000 to 2800 cm^{-1}) and the slight peak-shift toward lower wavenumbers as well as the change in intensity caused by the hydrolysis. In the middle region of the spectrum (1800 to 1350 cm^{-1}; Fig. 1C), drastic spectral changes can be observed, with an overall decrease in intensity and band broadening of the νCO, the concomitant apparition of the νCOO^- and some changes on the $\nu_{sci}CH_2$. Within the 1150 to 1000 cm^{-1} region (Fig. 1D), the head-group vibrations also present some changes, *i.e.* an overall shift toward lower wavenumbers and changes in the relative intensities of the 1090 and 1060 cm^{-1} subcomponents. Since the changes occurring at the νCO and νCOO^- region are more intense and less affected by the contributions of other vibrations, we focused on the analysis of this portion of the IR spectrum during the hydrolysis.

3.2. Changes occurring in carbonyl and carboxylate stretching vibrations

The interfacial carbonyl group is highly implicated in the chemical events occurring during DPPC hydrolysis and thus it is not surprising that the most striking spectral changes are detected at the CO and COO^- stretching regions (Fig. 1C). The most specific spectral feature that can be directly related to the action of GPLRP2 on DPPC is the decrease in the intensity of the band around 1735 cm^{-1} that can be attributed to the decrease in the concentration of the DPPC and other diacyl glycerophospholipids (Gericke and Huhnerfuss, 1994; Grandbois et al., 1999, 2000). The second most striking spectral change is the increase in the intensity around 1700 cm^{-1}, which has been associated with protonated fatty acids (O'connor and Cleverly, 1994; Poulsen et al., 2005). The global effect of these relative intensity changes is the observed CO stretching shift toward lower wavenumbers and band broadening indicating an overall increase in CO group populations with higher degree of H-bonding and hydration (Hubner and Blume, 1998; Lewis et al., 1994). The third most prominent feature is the appearance of a doublet around 1576 and 1538 cm^{-1}, that can be assigned to the asymmetric carboxylate stretching (Kimura et al., 1986; Oomens and Steill, 2008). All these combined changes in the IR spectrum give information about the substrate consumption and the release of hydrolysis products. Fig. 2 shows in more detail the changes occurring in the νCO and νCOO^- region (1800 to 1500 cm^{-1}) directly in the raw spectra (panels A and B) as well as in the difference spectra (panels C and D) at pD 6 and 8 during 120-min hydrolysis by GPLRP2. At both pD-values, the higher frequency subcomponent (around 1735 cm^{-1}) of the νCO decreases in intensity, which corresponds to DPPC hydrolysis, while the lower frequency subcomponent (around 1700 cm^{-1}) increases, which corresponds to the production of protonated fatty acids. These changes are stronger at pD 8 than pD 6. At pD 6, however, the decrease in the intensity at 1735 cm^{-1} equals the increase observed at 1700 cm^{-1}, while at pD 8 the increase in intensity at 1700 cm^{-1} is almost a third of the decrease observed at 1735 cm^{-1}. We also observe that the peak at 1735 cm^{-1} shifts toward higher wavenumbers during the hydrolysis at pD 8. The carboxylate stretching vibration (νCOO^-; doublet at 1576 and 1538 cm^{-1} doublet) is seen at pD 8 but not at pD 6, which indicates that the palmitic acid released during the hydrolysis reaction is not ionized at pD 6. This finding is consistent with the high pKa values measured for long chain fatty acids (Kanicky et al., 2000; Kanicky and Shah, 2003). Therefore, studying νCOO^- variations is only relevant for experiments at pD 8, at which long chain fatty acids are largely ionized, while they are fully protonated at pD 6. For this reason, we decided to focus only on changes occurring at the νCO for further analysis of DPPC hydrolysis.

3.3. Calibration of IR absorbance versus concentration of DPPC, lysoPC and pam standards

To estimate the concentrations of the residual substrate and released products during the hydrolysis of DPPC-NaTDC micelles, we first established a calibration of IR absorbance versus concentration using dispersions of individual compounds (DPPC, lysoPC or Pam) in mixed micelles with 50 mM NaTDC, at 35 °C. Fig. 3 shows the νCO of these dispersions at pD 6 and 8, at concentrations ranging from 0 to 10% w/v (≈ 0 to 130 mM) for DPPC, from 0 to 5% w/v (≈0 to 100 mM) for lysoPC and from 0 to 5% w/v (0 to 195 mM) for Pam.

Maximum absorptions are observed at different wavenumbers for DPPC (1735 cm^{-1}), lysoPC (1725 cm^{-1}) and Pam (1700 cm^{-1}), as indicated by dotted lines in Fig. 3. The line-shapes of the spectra are also different, with DPPC νCO being slightly asymmetric compared to lysoPC νCO. While DPPC and lysoPC νCO spectra are not significantly different at pD 6 and 8, the Pam νCO spectra are highly dependent on the pD-value, being more narrow and asymmetric at pD 6 and wider and symmetric at pD 8 and high concentrations. Other interesting observations are the concentration-dependent peak-shifts observed

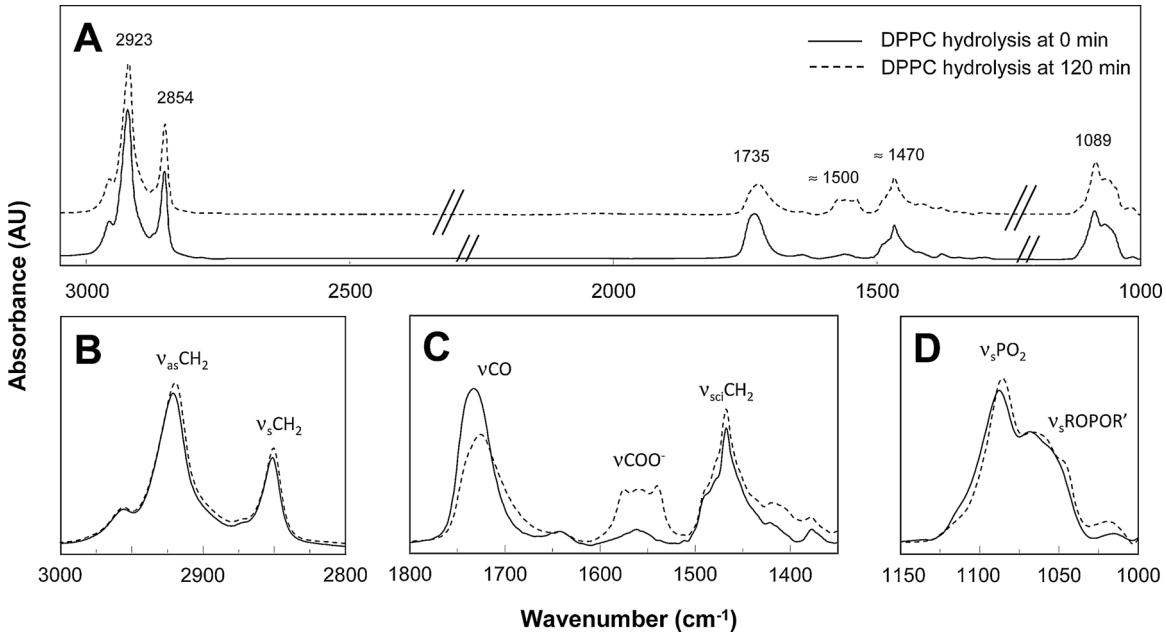

Fig. 1. *Representative IR spectra of DPPC-NaTDC micelles before and after 120 minutes of hydrolysis by GPLRP2 at 35 °C and pD 8.* Panel A: whole IR spectrum after D_2O buffer subtraction, H_2O vapor and baseline correction. Panel B: CH stretching vibrations, mainly the asymmetric ($\nu_{as}CH_2$) and symmetric (ν_sCH_2) methylene vibrations. Panel C: region corresponding to the CO and COO^- stretching vibrations (νCO and νCOO^-) as well as to the CH scissoring bending ($\nu_{sci}CH_2$). Panel D: head-group vibrations, mainly the symmetric PO_2 and ROPOR' stretching vibrations (ν_sPO_2 and ν_sROPOR').

towards lower wavenumbers for Pam νCO at pD 8, and towards higher wavenumbers for DPPC νCO at both pD-values.

We selected the IR absorbance at wavenumbers of 1735, 1726 and 1700 cm^{-1} to establish calibration curves from individual dispersions of pure DPPC (Fig. S1 in Supplementary data), lysoPC (Fig. S2) and Pam (Fig. S3). For each compound and pD value, three molar extinction coefficients (ε, $M^{-1}\,cm^{-1}$) were estimated from IR absorbance at the selected wavenumbers (Table 1). For each wavenumber, the ε-value corresponds to the slope of the linear regression line established from the scatterplot of IR absorbance versus compound concentration (see Figs. S1, S2 and S3 in Supplementary data). Indeed, we observed in all cases that IR absorbance varies linearly with the concentration as indicated by the very good coefficients of determination r^2 obtained from linear regression (Table 1).

For both DPPC and lysoPC, the ε − values are similar at pD 6 and 8, while in contrast, those of Pam are highly pD-dependent. There is a lack of absorption of Pam at 1735 and 1726 cm^{-1} at pD 6, while slight absorptions are observed at pD 8 with ε − values of 34 $M^{-1}cm^{-1}$ at 1735 cm^{-1} and 47 $M^{-1}cm^{-1}$ at 1726 cm^{-1}. Pam is the component that presents, however, the highest molar absorption coefficient at 1700 cm^{-1} (115 $M^{-1}cm^{-1}$), followed by lysoPC (102 $M^{-1}cm^{-1}$) and DPPC (50 $M^{-1}cm^{-1}$).

3.4. Estimation of DPPC, lysoPC and pam concentrations in hydrolysis reaction mixtures using IR absorbance

Using the molar absorption coefficients estimated from calibration curves and the IR spectra recorded during the time-course hydrolysis of DPPC, it was possible to estimate the concentration of each compound by solving a 3 × 3 equation system. This estimation assumes that (i) the absorbance of the DPPC hydrolysis mixture at a given wavenumber results from the sum of the absorbances of DPPC, lysoPC and Pam, and (ii) the absorbance varies linearly with the concentration for each compound (as observed in calibration curves; Figs. S1, S2 and S3), *i.e.*

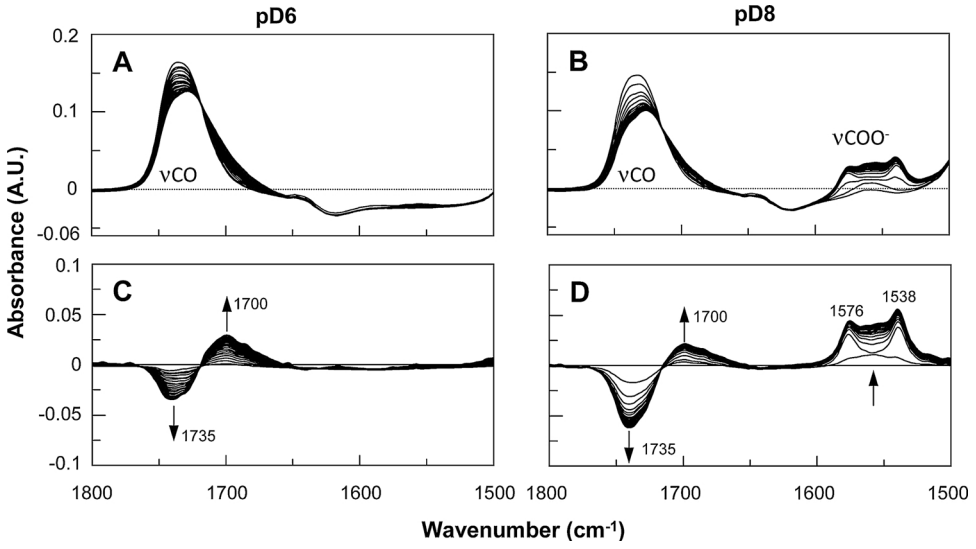

Fig. 2. *IR spectra of CO and COO^- stretching vibrations during the hydrolysis of DPPC-NaTDC micelles by GPLRP2.* Panels A and B show the evolution of the 'raw' spectra at pD 6 and 8, respectively, while panels C and D show the difference spectra at pD 6 and 8, respectively, obtained from the subtraction of the initial IR spectrum. DPPC hydrolysis was monitored for 120 min at 5-min intervals, at 35 °C. GPLRP2 concentration was 100 nM.

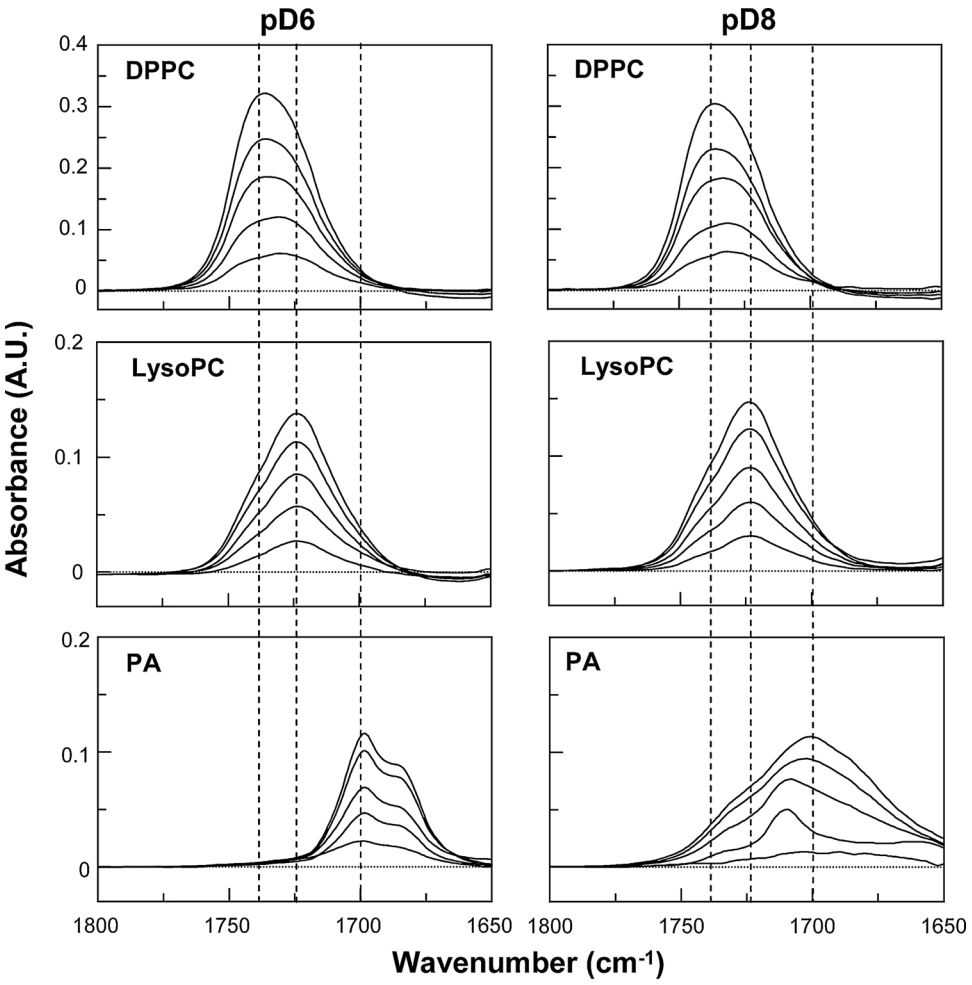

Fig. 3. *IR spectra of CO stretching vibration of DPPC, lysoPC and Pam at different concentrations in presence of 50 mM of NaTDC.* The lipid concentrations range from 0 to 10% w/v (≈ 0 to 130 mM) for DPPC, from 0 to 5% w/v (≈0 to 100 mM) for lysoPC and from 0 to 5% w/v (0 to 195 mM) for Pam. IR spectra were recorded at 35 °C and pD 6 (left-side panels) and pD 8 (right-side panels). Vertical dashed lines indicate relevant wavenumbers: 1735, 1726 and 1700 cm^{-1}.

Table 1
Molar extinction coefficients (ε, M^{-1} cm^{-1}) of DPPC, lysoPC and Pam estimated from IR absorbance. The ε-values represent the slope of the standard calibration curves of IR absorbance of DPPC, lysoPC and Pam measured at 1735, 1726 and 1700 cm^{-1}, at pD 6 and pD 8 (see Figs. S2, S3 and S4 in Supplementary data). All IR measurements were performed in D_2O, in the presence of 50 mM NaTDC, and at 35 °C.

Wavenumber	Compound	pD 6		pD8	
		ε	r^2	ε	r^2
1735 cm^{-1}	DPPC	482.0	0.997	484.9	0.996
	LysoPC	227.3	0.992	215.6	0.997
	Pam	0	0	34.2	0.998
1726 cm^{-1}	DPPC	415.0	0.999	417.6	0.998
	LysoPC	303.0	0.996	287.4	0.999
	Pam	0	0	47.4	0.993
1700 cm^{-1}	DPPC	53.2	0.955	42.9	0.920
	LysoPC	102.5	0.984	94.8	0.998
	Pam	120.5	0.995	113.2	0.996

that intermolecular interactions have no major impact on the IR spectrum and can be neglected (see further discussion in section 3.6).

For each reaction and time point, IR absorbance at 1735, 1726 and 1700 cm^{-1} were extracted from the IR spectrum and used in the following system of 3 equations with 3 unknowns to estimate DPPC, lysoPC and Pam concentrations:

$$A_{1735} = \varepsilon_{DPPC}^{1735}[DPPC] + \varepsilon_{lysoPC}^{1735}[lysoPC] + \varepsilon_{PA}^{1735}[PA] \quad (1)$$

$$A_{1726} = \varepsilon_{DPPC}^{1726}[DPPC] + \varepsilon_{lysoPC}^{1726}[lysoPC] + \varepsilon_{PA}^{1726}[PA] \quad (2)$$

$$A_{1700} = \varepsilon_{DPPC}^{1700}[DPPC] + \varepsilon_{lysoPC}^{1700}[lysoPC] + \varepsilon_{PA}^{1700}[PA] \quad (3)$$

where A_i is the absorbance at the wavenumber 'i', ε_x^i is the molar extinction coefficient of the compound 'x' at the wavenumber 'i' and [x] is the concentration of the compound 'x', which is DPPC, lysoPC or Pam. This equation system can be written as the following 3 × 3 matrix system:

$$\begin{bmatrix} A_{1735} \\ A_{1726} \\ A_{1700} \end{bmatrix} = \begin{bmatrix} \varepsilon_{DPPC}^{1735} & \varepsilon_{lysoPC}^{1735} & \varepsilon_{PA}^{1735} \\ \varepsilon_{DPPC}^{1726} & \varepsilon_{lysoPC}^{1726} & \varepsilon_{PA}^{1726} \\ \varepsilon_{DPPC}^{1700} & \varepsilon_{lysoPC}^{1700} & \varepsilon_{PA}^{1700} \end{bmatrix} \times \begin{bmatrix} [DPPC] \\ [lysoPC] \\ [PA] \end{bmatrix} \quad (4)$$

which can be further represented as follows:

$$A = E \cdot C \quad (5)$$

$$C = E^{-1} \cdot A \quad (6)$$

where A and C are the absorbance and concentration column vectors, respectively, and E^{-1} is the inversed of the molar extinction coefficient 3 × 3 matrix. Eq. (6) allows the estimation of DPPC, lysoPC and Pam concentrations from IR absorbance at 1735, 1726 and 1700 cm^{-1}.

The time-dependent variations in DPPC, lysoPC and Pam concentrations resulting from DPPC hydrolysis by GPLRP2 and deduced from IR spectra are shown in Figs. 4A (pD 6) and 4 B (pD 8). Whatever the pD-value, a very good correlation is observed between the consumption of DPPC and the appearance of Pam, as indicated by the Pam to hydrolyzed DPPC molar ratio that remains close to 1 during the whole hydrolysis reaction (1.02 ± 0.09 at pD 6 and 0.84 ± 0.06 at pD 8; see Fig. S5 in Supplementary data). This finding also indicates

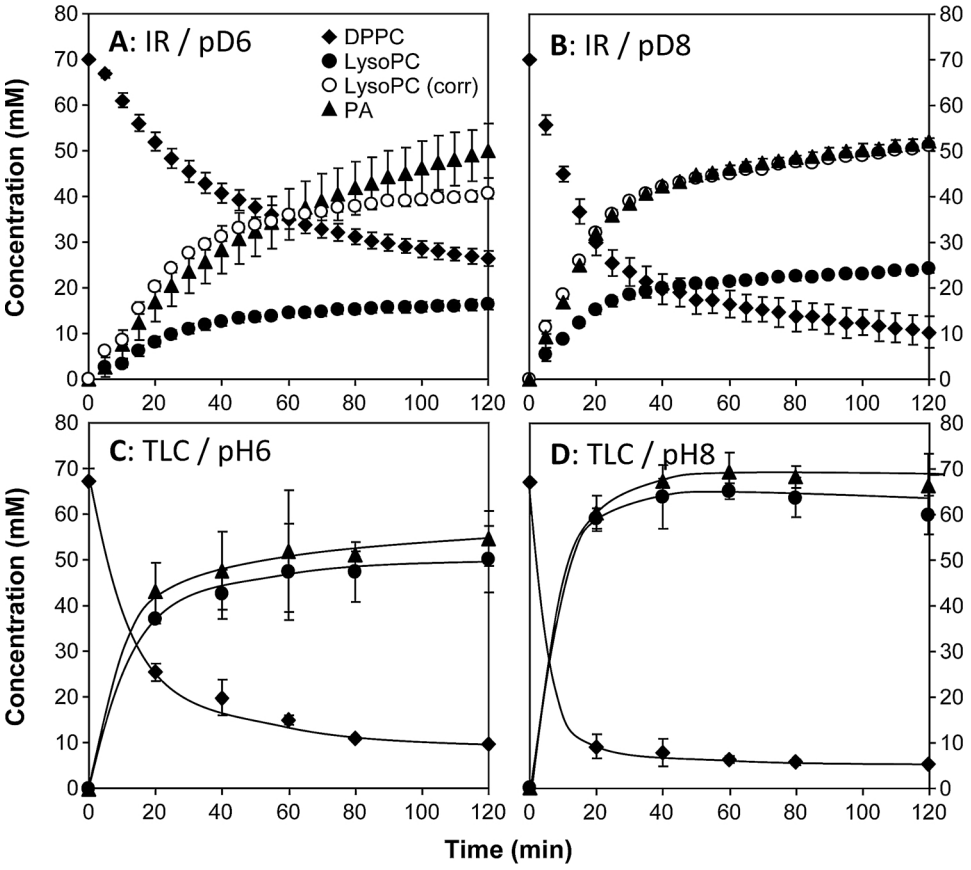

Fig. 4. *Time-course variations in lipolysis products during the hydrolysis of DPPC-NaTDC micelles by GPLRP2.* Experiments monitored by IR spectroscopy were performed at pD 6 (panel A) and 8 (panel B), at 35 °C for 120 min. IR spectra were recorded every 5 min. Experiments monitored by TLC analysis were performed at pH 6 (panel C) and 8 (panel D), at 35 °C for 120 min. Samples for extraction of lipolysis products and TLC analysis were collected every 20 min. GPLRP2 concentration was 100 nM in both series of experiments. Values are means ± SD (n = 3).

Table 2
Comparison of GPLRP2 specific activities (U/mg) on DPPC-NaTDC micelles estimated from IR spectrum analysis, TLC and pH-stat titrimetric assay. Experiments were performed in triplicate in D_2O or H_2O depending on the assay, at pD/pH 6 and 8, at 35 °C.

Method	pD 6/pH 6	pD 8/pH 8	pH 8 to pH 6 ratio
IR (D_2O)	192.6 ± 53.2	305.1 ± 23.9	1.58
TLC (H_2O)	432.9 ± 62.4	628.1 ± 38.1	1.45
D_2O/H_2O ratio (IR vs. TLC)	0.44	0.49	
pH-Stat (D_2O)	317.0 ± 17.7	439.7 ± 13.5	1.39
pH-Stat (H_2O)	575.2 ± 54.2	889.0 ± 40.8	1.55
D_2O/H_2O ratio (pH-stat)	0.55	0.49	

that only one ester bond of DPPC is cleaved by GPLRP2, presumably at the *sn*-1 position, during these experiments, although some activity of GPLRP2 on the *sn*-2 position has been reported (El Alaoui et al., 2016). From the variations in DPPC and Pam concentrations, we could estimate the conversion level of DPPC into lysoPC, that reached 50% after 60 min at pD 6 and after 15 min at pD 8. The conversion level reached after 120 min of reaction was 62.1 ± 2.3% at pD 6 and 85.3 ± 4.9% at pD 8. We also estimated the initial specific activity of GPLRP2 from the quasi linear increase in Pam concentration observed for $t \leq 20$ min. Under the condition of the IR spectroscopy assay, GPLRP2 specific activity on DPPC was found to be 192.6 ± 53.2 U/mg at pD 6 and 305.1 ± 23.9 U/mg at pD 8 (Table 2), with 1 U = 1 µmole of Pam released per min.

We observed, however, that the apparent lysoPC concentration calculated from the IR spectra was about the half of that expected from DPPC disappearance and Pam release. This difference may be explained by the effect of intermolecular interactions in the hydrolysis mixture, but also by a difference in the molar absorption coefficients of the lysoPC used as standard here (1-lysoPC) and the lysoPC released during the hydrolysis (2-lysoPC resulting from the PLA1 activity of GPLRP2). This latter hypothesis is the most probable since the carbonyl groups in 1-lysoPC and 2-lyso-PC are found in very different intramolecular environments and one can expect distinct C=O stretching vibrations for these compounds (Eibl and Lands, 1970). The choice of 1725 cm^{-1} as the wavenumber corresponding to the maximum absorbance of lysoPC in the C=O stretching region will have to be re-evaluate with a more relevant standard. It is however quite difficult to obtain relatively pure 1-hydroxy-2-palmitoyl-*sn-glycero*-3-phosphocholine (2-lysoPC) from DPPC hydrolysis reactions since isomerization into 1-lysoPC occurs rapidly, with an equilibrium mixture of 90% 2-lysoPC and 10% 1-lysoPC obtained in about 10 min at the pH/pD we used (Croset et al., 2000; Pluckthun and Dennis, 1982). The only possibility to prepare relatively pure 1-lysoPC is to synthesize it (Eibl and Lands, 1970) and to keep it in organic solvent or dry. IR spectra recorded under these conditions might be however quite different from those recorded in solution, where hydration and hydrogen bonds have a major impact.

Nevertheless, correction factors for lysoPC levels could be established from the ratio of Pam to apparent lysoPC molar concentrations, based on the fact that no further hydrolysis of lysoPC by GPLRP2 occurs in our experiments and that the Pam to lysoPC molar ratio should be equal to 1. Since the Pam to apparent lysoPC ratio remained almost constant throughout the hydrolysis reaction, we could calculate global correction factors of 2.5 ± 0.5 at pD 6 and 2.1 ± 0.1 at pD 8. The variations in the "corrected" lysoPC concentration were then plotted in Figs. 4A and 4B.

3.5. Comparison of IR spectroscopy with TLC and pHstat titration to monitor DPPC hydrolysis and estimate GPLRP2 specific activity

To validate the IR spectroscopy analysis of DPPC hydrolysis and the lipolysis product concentrations deduced from this analysis, we

performed similar hydrolysis experiments at pH 6 and pH 8 that were further analyzed by TLC coupled to densitometry (see Fig. S4 in Supplementary data). Overall, the DPPC, Pam and lysoPC concentrations were in the same ranges, but the kinetics of hydrolysis were different (Figs. 4C and 4D), DPPC conversion estimated from TLC analysis was faster and reached 50% after around 15 min at pH 6 and 5–10 min at pH 8. The conversion level reached after 120 min of reaction was 85.6 ± 5.7% at pH 6 and 95.5 ± 4.5% at pD 8. Higher levels of Pam were initially observed and the specific activity of GPLRP2 estimated from TLC analysis (432.9 ± 62.4 U/mg at pH 6 and 628.1 ± 38.1 U/mg at pH 8; Table 2) was around 2-fold higher than that deduced from IR spectroscopy assays (Table 2).

Since the lipolysis experiments monitored by IR spectroscopy were performed in D_2O and those monitored by TLC in water, we assumed that the differences observed in the lipolysis rates and GPLRP2 specific activities resulted from these solvents with distinct dissociation properties and impacts on the pH value. We therefore assessed the specific activity of GPLRP2 on the DPPC-NaTDC mixed micelles prepared in both D_2O and water using another method based on titrimetry, the pH-stat method (Table 2). Titration was performed with 0.1 M NaOH and pH endpoint values were fixed at pH 6 or pH 8 in both cases. The specific activities of GPLRP2 on DPPC micelles prepared in D_2O were 317 ± 17.7 and 439.7 ± 13.5 U/mg at pH 6 and 8, respectively, while they were around 2-fold higher on DPPC micelles prepared in H_2O (575.2 ± 54.2 and 889.0 ± 40.8 U/mg at pH 6 and 8, respectively). We therefore confirmed that GPLRP2 activity in D_2O is lower than in water, and this can explain the differences observed between IR spectroscopy and TLC experiments. One will have to take it into account for future hydrolysis experiments monitored by IR spectroscopy in D_2O. Nevertheless, an interesting finding is that the pD 6/pD 8 and D_2O/H_2O activities ratios are conserved regardless of the method used to determine the enzymatic activity of GPLPR2 (Table 2).

3.6. Additivity of individual compound absorbances and possible impact of intermolecular interactions on CO stretching vibrations

To better explore the changes occurring at the CO stretching subcomponents during the hydrolysis, the νCO spectra before and after 20 min of reaction with GPLRP2 at pD 8 were deconvolved and compared (Fig. 5). One can observe that the overall intensity decreased and band broadening is the result of changes in the relative intensities of the νCO subcomponents. The main effect of the hydrolysis is the decrease in intensity of higher frequency subcomponents and the apparition of various subcomponents at lower wavenumbers that can be assigned to the formation of the reaction products (lysoPC and Pam). To reproduce these effects, we prepared a mixed dispersion (Mix) containing the amounts of DPPC, lysoPC and Pam estimated after 20-min hydrolysis of DPPC at pD 8 (Fig. 4B) and corresponding to around 50% conversion of DPPC, as well as a reconstructed spectrum (Rec) obtained by combining the individual spectra of pure DPPC, lysoPC and Pam, with an arithmetic adjustment of their intensities mimicking the hydrolysis mixture obtain at 20 min at pD 8. We observed that the IR spectrum recorded after 20 min of hydrolysis overlaps almost completely with the spectrum of the mixed dispersion and the reconstructed spectrum. This reconstruction supports the assumption that DPPC, lysoPC and Pam display similar vibrational properties when they are alone and when they are present in a mixture, and validate the approach used for quantifying individual molecular species from the complex IR spectra recorded during DPPC hydrolysis. Whatever the nature and intensity of intermolecular interactions, they do not seem to perturb significantly the linearity of the standard calibration curves nor the additivity of individual compound absorbances in the complex mixture resulting from DPPC hydrolysis. It is worth noticing, however, that the presence of some concentration-dependent peak-shifts and asymmetries in the case of DPPC and Pam νCO (Fig. 3) suggest complex intermolecular interactions. These concentration-dependent changes in the vibration

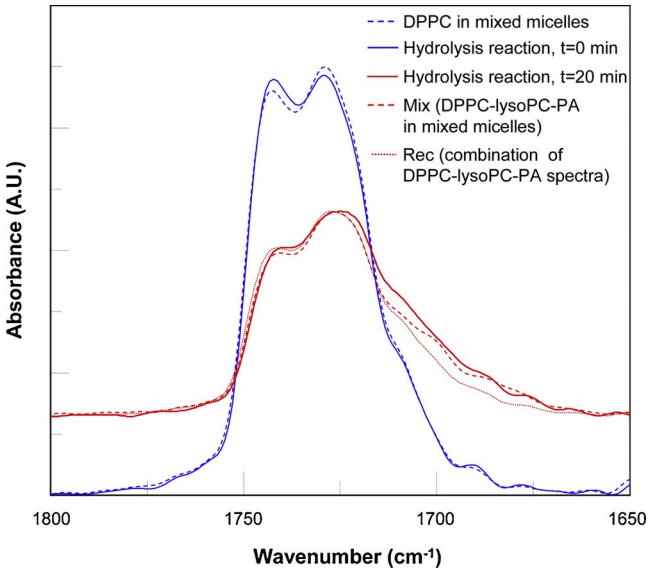

Fig. 5. *Deconvolved IR spectra of CO stretching vibration of DPPC-NaTDC micelles before and after 20 min of hydrolysis by 100 nM GPLRP2 at pD 8.* The spectrum at t = 0 min of hydrolysis was compared to that of pure DPPC-NaTDC micelles. The spectrum recorded after 20 min of hydrolysis was compared to that of a mixture (mix) of DPPC, lysoPC and Pam at their respective concentrations estimated for 50% of hydrolysis (≈35 mM for the 3 compounds) and to a reconstructed spectrum (rec) built after addition and arithmetic adjustment of the individual spectra of DPPC, lysoPC and Pam recorded in the presence of NaTDC.

frequencies in this spectral region could result from variations in the interfacial H-bonding and hydration, possibly due to changes in the micellar structure, lipid conformation and lyotropic mesomorphism (Danielsson et al., 1976). Other systematic experiments using various mixtures of lipolysis products should be done to better assess the intermolecular interaction arising from the mixing.

3.7. Other informations from IR spectroscopy on physicochemical changes occurring during the hydrolysis of DPPC-NaTDC micelles

Upon the hydrolysis reaction, we observed changes in the CH stretching region (Fig. 1B) suggesting an overall increase of the hydrophobic acyl chains conformational order and a decrease of the librotorsional mobility in the presence of lipolysis products. However, we have to be careful with straightforward interpretations of peak-shifts and band broadenings in this region, due to the presence of more than one chemical compound containing CH_2 groups and quite similar chemical structures, since this may result in possible combination, resonance and/or coupling effects (Kodati et al., 1994; Snyder et al., 1978). Other drawback concerning the CH stretching vibrations analysis during lipid hydrolysis is that in phospholipid and fatty acid molecules there are several “populations” of CH_2 groups that might display slightly different vibrational properties and thus resulting in the averaging of all these effects on the final observed spectra. Nevertheless, it would be worth completing this study by independent experiments on the physical-chemical characterization of the colloidal mixture during lipolysis to eventually correlate changes in the CH stretching region of the IR spectra with structural changes in lipid aggregates/micelles.

The interpretation of the symmetric PO and the ROPOR stretching vibrations (Fig. 1C) is not straightforward either. However, based on previous observations on pure phospholipid-surfactant systems (Goñi and Arrondo, 1986; Goñi et al.,1986), the changes observed after DPPC hydrolysis indicates an overall change in the phosphate head-group hydration, H-bonding patterns and orientations. The presence of more than one chemical compound containing similar phosphate groups in the hydrolysate (DPPC, lysoPC and possibly some glycerophosphocholine) and the possible effects of vibrational contributions other than

those of the phosphate groups (Fringeli and Gunthard, 1981; Mendelsohn and Mantsch, 1985) further complicates the analysis.

4. Conclusions

Infrared spectroscopy is a versatile tool that allows the study of very dynamic and complex systems such as biological samples in which protein-lipid interactions occur. We previously showed how transmission IR spectroscopy could be used to investigate in bulk the interaction of a phospholipase, GPLRP2, with various phospholipid dispersions (Mateos-Diaz et al., 2017). We extended this investigation with the active enzyme to explore the subsequent step of substrate hydrolysis using phospholipid-bile salt mixed micelles. Assuming that the DPPC substrate and lipolysis products display similar vibrational properties when they are alone in a dispersion and when they are present as a mixture during the hydrolysis, IR spectroscopy allows monitoring continuously the phospholipid hydrolysis, with the quantification of residual substrate and all lipolysis products, the determination of enzyme activity and even to obtain some information on the acyl chain packing, interfacial hydration and H-bonding in situ in the course of the lipolysis reaction. This contrasts with other methods that require lipid extraction or laborious preparation of supported lipid films. The results we obtained are coherent with hydrolysis and lipolysis product levels obtained in parallel experiments using TLC quantification and titrimetric pH stat assay, although enzyme kinetics in D_2O are slower from those recorded in water. In summary, we have shown that it is possible to use IR spectroscopy to have a quite complete hydrolysis profile and even some information of physicochemical variations of the substrate. We can envisage to use this method with other lipid substrates and lipolytic enzymes.

Conflict of interest

All authors declare no conflict of interest.

Contributions

Dr Eduardo Mateos-Diaz was involved in the conception and design of the study, in acquisition, analysis and interpretation of data on protein production, FTIR spectroscopy and enzyme assays, in drafting the article, revising it critically for important intellectual content. Dr Priscila Sutto-Ortiz was involved in the acquisition, analysis and interpretation of data related to phospholipid hydrolysis and thin layer chromatography, as well as in drafting the article. Moulay Sahaka, MSc, was involved in the acquisition, analysis and interpretation of data related to FTIR spectroscopy. Dr Jorge Rodriguez was involved in drafting and revising the article for important intellectual contents. Dr Frédéric Carrière was involved in the conception and design of the study, in drafting the article, revising it critically for important intellectual content and final approval of the version to be submitted. All authors were involved in the final approval of the version to be submitted.

Acknowledgements

Eduardo Mateos-Diaz and Priscila Sutto-Ortiz are grateful to CONACYT for the financial support received during their PhD thesis (scholarships ID 217854/313389 for E.M.D. and 376598/247081 for P.S.O). Moulay Sahaka is grateful to Aix Marseille Université for his PhD scholarship. This work was supported by Centre National de la Recherche Scientifique.

References

Ackman, R.G., McLeod, C.A., Banerjee, A.K., 1990. An overview of analyses by Chromarod-Iatroscan TLC-FID. J. Planar Chromatog. 3, 450–462.

Amara, S., Lafont, D., Fiorentino, B., Boullanger, P., Carriere, F., De Caro, A., 2009. Continuous measurement of galactolipid hydrolysis by pancreatic lipolytic enzymes using the pH-stat technique and a medium chain monogalactosyl diglyceride as substrate. Biochim. Biophys. Acta-Mol. Cell Biol. Lipids 1791, 983–990.

Beisson, F., Ferte, N., Nari, J., Noat, G., Arondel, V., Verger, R., 1999. Use of naturally fluorescent triacylglycerols from Parinari glaberrimum to detect low lipase activities from Arabidopsis thaliana seedlings. J. Lipid Res. 40, 2313–2321.

Beisson, F., Tiss, A., Rivière, C., Verger, R., 2000. Methods for lipase detection and assay: a critical review. Eur. J. Lipid Sci. Technol. 2, 133–153.

Brockman, H.L., 1981. Triglyceride lipase from porcine pancreas. Methods Enzymol. 71 (Pt. C), 619–627.

Camacho-Ruiz Mde, L., Mateos-Diaz, J.C., Carriere, F., Rodriguez, J.A., 2015. A broad pH range indicator-based spectrophotometric assay for true lipases using tributyrin and tricaprylin. J. Lipid Res. 56, 1057–1067.

Cavalier, J.F., Lafont, D., Boullanger, P., Houisse, D., Giallo, J., Ballester, J.M., Carriere, F., 2009. Validation of lipolysis product extraction from aqueous/biological samples, separation and quantification by thin-layer chromatography with flame ionization detection analysis using O-cholesteryl ethylene glycol as a new internal standard. J. Chromatogr. A 1216, 6543–6548.

Croset, M., Brossard, N., Polette, A., Lagarde, M., 2000. Characterization of plasma unsaturated lysophosphatidylcholines in human and rat. Biochem. J 345 (Pt. 1), 61–67.

Danielsson, I., Rosenholm, J.B., Stenius, P., Backlund, S., 1976. Lyotropic mesomorphism and aggregation in surfactant systems. Colloids and Surfaces: Selected Plenary Lectures of the IUPAC-Conference on Colloid and Surface Science in Budapest, September 15â€20, 1975. Steinkopff, Darmstadt, pp. 1–11.

Dennis, E.A., 1973. Kinetic dependence of phospholipase A 2 activity on the detergent Triton X-100. J. Lipid Res. 14, 152–159.

Desnuelle, P., Constantin, M.J., Baldy, J., 1955. Technique potentiométrique pour la mesure de l'activité de la lipase pancréatique. Bull. Soc. Chim. Biol. (Paris) 37, 285–290.

Eibl, H., Lands, W.E.M., 1970. Phosphorylation of 1-alkenyl-2-acylglycerol and preparation of 2-acylphosphoglycerides. Biochemistry 9, 423–428.

El Alaoui, M., Soulere, L., Noiriel, A., Popowycz, F., Khatib, A., Queneau, Y., Abousalham, A., 2016. A continuous spectrophotometric assay that distinguishes between phospholipase A1 and A2 activities. J. Lipid Res. 57, 1589–1597.

Feng, L., Manabe, K., Shope, J.C., Widmer, S., DeWald, D.B., Prestwich, G.D., 2002. A real-time fluorogenic phospholipase A(2) assay for biochemical and cellular activity measurements. Chem. Biol. 9, 795–803.

Fringeli, U.P., Gunthard, H.H., 1981. Infrared membrane spectroscopy. Mol. Biol. Biochem. Biophy. 31, 270–332.

Gargouri, Y., Piéroni, G., Rivière, C., Saunière, J.-F., Lowe, P.A., Sarda, L., Verger, R., 1986. Kinetic assay of human gastric lipase on short- and long-chain triacylglycerol emulsions. Gastroenterology 91, 919–925.

Gericke, A., Huhnerfuss, H., 1994. IR reflection-absorption spectroscopy – a versatile tool for studying interfacial enzymatic processes. Chem. Phys. Lipids 74, 205–210.

Goñi, F.M., Arrondo, J.L.R., 1986. A study of phospholipid phosphate groups in model membranes by Fourier transform infrared spectroscopy. Faraday Discuss 81, 117–126.

Goñi, F.M., Urbaneja, M.A., Arrondo, J.L.R., Alonso, A., Durrani, A.A., Chapman, D., 1986. The interaction of phosphatidylcholine bilayers with Triton X-100. Eur. J. Biochem. 160, 659–665.

Grandbois, M., Desbat, B., Blaudez, D., Salesse, C., 1999. Polarization-modulated infrared reflection absorption spectroscopy measurement of phospholipid monolayer hydrolysis by phospholipase C. Langmuir 15, 6594–6597.

Grandbois, M., Desbat, B., Salesse, C., 2000. Monitoring of phospholipid monolayer hydrolysis by phospholipase A2 by use of polarization-modulated Fourier transform infrared spectroscopy. Biophys. Chem. 88, 127–135.

Heinze, M., Roos, W., 2013. Assay of phospholipase A activity. Methods Mol. Biol. 1009, 241–249.

Hubner, W., Blume, A., 1998. Interactions at the lipid-water interface. Chem. Phys. Lipids 96, 99–123.

Kanicky, J.R., Shah, D.O., 2003. Effect of premicellar aggregation on the pKa of fatty acid soap solutions. Langmuir 19, 2034–2038.

Kanicky, J.R., Poniatowski, A.F., Mehta, N.R., Shah, D.O., 2000. Cooperativity among molecules at interfaces in relation to various technological processes: effect of chain length on the pKa of fatty acid salt solutions. Langmuir 16, 172–177.

Kennedy, D.F., Slotboom, A.J., Dehaas, G.H., Chapman, D., 1990. A Fourier transform infrared spectroscopic (FTIR) study of porcine and bovine pancreatic phospholipase A2 and their interaction with substrate analogs and a transition-state inhibitor. Biochim. Biophys. Acta 1040, 317–326.

Kimura, F., Umemura, J., Takenaka, T., 1986. FTIR-ATR studies on Langmuir-Blodgett films of stearic acid with 1–9 monolayers. Langmuir 2, 96–101.

Kodati, V.R., Eljastimi, R., Lafleur, M., 1994. Contribution of the intermolecular coupling and librotorsional mobility in the methylene stretching modes in the infrared-spectra of acyl chains. J. Phys. Chem. 98, 12191–12197.

Kwon, D.Y., Rhee, J.S., 1986. A simple and rapid colorimetric method for determination of free fatty acids for lipase assay. JAOCS 63, 89–92.

Labourdenne, S., Gaudry-Rolland, N., Letellier, S., Lin, M., Cagna, A., Esposito, G., Verger, R., Rivière, C., 1994. The oil-drop tensiometer: potential applications for studying the kinetics of (phospho)lipase action. Chem. Phys. Lipids 71, 163–173.

Lefevre, T., Subirade, M., 2000. Interaction of beta-lactoglobulin with phospholipid bilayers: a molecular level elucidation as revealed by infrared spectroscopy. Int. J. Biol. Macromol. 28, 59–67.

Lewis, R.N.A.H., McElhaney, R.N., 2013. Membrane lipid phase transitions and phase organization studied by Fourier transform infrared spectroscopy. Biochim. Biophys. Acta-Biomembr. 1828, 2347–2358.

Lewis, R., McElhaney, R.N., Pohle, W., Mantsch, H.H., 1994. Components of the carbonyl stretching band in the infrared-spectra of hydrated 1,2-diacylglycerolipid bilayers – a reevaluation. Biophys. J. 67, 2367–2375.

Mateos-Diaz, E., Rodriguez, J.A., de Los, Angeles, Camacho-Ruiz, M., Mateos-Diaz, J.C., 2012. High-throughput screening method for lipases/esterases. Methods Mol. Biol. 861, 89–100.

Mateos-Diaz, E., Bakala N'Goma, J.C., Byrne, D., Robert, S., Carriere, F., Gaussier, H., 2017. IR spectroscopy analysis of pancreatic lipase-related protein 2 interaction with phospholipids: 1. Discriminative recognition of mixed micelles versus liposomes. Chem. Phys. Lipids.

Mendelsohn, R., Mantsch, H.H., 1985. Fourier transform infrared studies of lipid-protein interactions. In: Watts, A., Pont, J.J.H.H.M.D. (Eds.), Progress in Protein-Lipid Interactions. Elsevier, Amsterdam, pp. 1103–1146.

Mendelsohn, R., Moore, D.J., 1998. Vibrational spectroscopic studies of lipid domains in biomembranes and model systems. Chem. Phys. Lipids 96, 141–157.

Mendoza, L.D., Rodriguez, J.A., Leclaire, J., Buono, G., Fotiadu, F., Carriere, F., Abousalham, A., 2012. An ultraviolet spectrophotometric assay for the screening of sn-2-specific lipases using 1,3-O-dioleoyl-2-O-alpha-eleostearoyl-sn-glycerol as substrate. J. Lipid Res. 53, 185–194.

Negre, A., Salvayre, R., Dousset, N., Rogalle, P., Dang, Q.Q., Douste-Blazy, L., 1988. Hydrolysis of fluorescent pyrenetriacylglycerols by lipases from human stomach and gastric juice. Biochim. Biophys. Acta 963, 340–348.

Nury, S., Pieroni, G., Riviere, C., Gargouri, Y., Bois, A., Verger, R., 1987. Lipase kinetics at the triacylglycerol-water interface using surface tension measurements. Chem. Phys. Lipids 45, 27–37.

O'connor, J., Cleverly, D.R., 1994. Fourier-transform infrared assay of bile salt-stimulated lipase activity in reversed micelles. J. Chem. Technol. Biotechnol. 61, 209–214.

Oomens, J., Steill, J.D., 2008. Free carboxylate stretching modes. J. Phys. Chem. A 112, 3281–3283.

Pencreac'h, G., Graille, J., Pina, M., Verger, R., 2002. An ultraviolet spectrophotometric assay for measuring lipase activity using long-chain triacylglycerols from Aleurites fordii seeds. Anal. Biochem. 303, 17–24.

Pluckthun, A., Dennis, E.A., 1982. Acyl and phosphoryl migration in lysophospholipids: importance in phospholipid synthesis and phospholipase specificity. Biochemistry 21, 1743–1750.

Poulsen, K.R., Snabe, T., Petersen, E.I., Fojan, P., Neves-Petersen, M.T., Wimmer, R., Petersen, S.B., 2005. Quantization of pH: Evidence for acidic activity of triglyceride Lipases. Biochemistry 44, 11574–11580.

Ransac, S., Moreau, H., Riviere, C., Verger, R., 1991. Monolayer techniques for studying phospholipase kinetics. Methods Enzymol. 197, 49–65.

Serveau-Avesque, C., Verger, R., Rodriguez, J.A., Abousalham, A., 2013. Development of a high-throughput assay for measuring lipase activity using natural triacylglycerols coated on microtiter plates. Analyst 138, 5230–5238.

Snabe, T., Petersen, S.B., 2002. Application of infrared spectroscopy (attenuated total reflection) for monitoring enzymatic activity on substrate films. J. Biotechnol. 95, 145–155.

Snyder, R.G., Hsu, S.L., Krimm, S., 1978. Vibrational spectra in C-H stretching region and structure of polymethylene chain. Spectrochim. Acta Part a-Mol. Biomol. Spectrosc. 34, 395–406.

Sutto-Ortiz, P., Camacho-Ruiz M. d. l.A. Kirchmayr, M.R., Camacho-Ruiz, R.M., Mateos-Diaz, J.C., Noiriel, A., Carriere, F., Abousalham, A., Rodriguez, J.A., 2017. Screening of phospholipase A activity and its production by new actinomycete strains cultivated by solid-state fermentation. Peer J. 5, e3524.

Tarvainen, M., J.P, S., Kallio, H., 2011. Ultra high performance liquid chromatography–mass spectrometric analysis of oxidized free fatty acids and acylglycerols. Eur. J. Lipid Sci. Technol. 113, 409–422.

Tatulian, S.A., Biltonen, R.L., Tamm, L.K., 1997. Structural changes in a secretory phospholipase A2 induced by membrane binding: a clue to interfacial activation? J. Mol. Biol. 268, 809–815.

Tatulian, S.A., 2001. Toward understanding interfacial activation of secretory phospholipase A(2) (PLA(2)): membrane surface properties and membrane-induced structural changes in the enzyme contribute synergistically to PLA(2) activation. Biophys. J . 80, 789–800.

Ulker, S., Placidi, C., Point, V., Gadenne, B., Serveau-Avesque, C., Canaan, S., Carriere, F., Cavalier, J.F., 2016. New lipase assay using Pomegranate oil coating in microtiter plates. Biochimie 120, 110–118.

Verger, R., de Haas, G.H., 1973. Enzyme reactions in a membrane model. 1: A new technique to study enzyme reactions in monolayers. Chem. Phys. Lipids 10, 127–136.

Verger, R., de Haas, G.H., 1976. Interfacial enzyme kinetics of lipolysis. Annu. Rev. Biophys. Bioeng. 5, 77–117.

Walde, P., Luisi, P.L., 1989. A continuous assay for lipases in reverse micelles based on Fourier transform infrared spectroscopy. Biochemistry 28, 3353–3360.

de Haas, G.H., Postema, N.M., Nieuwenhuisen, W., van Deenen, L.L.M., 1968. Purification and properties of phospholipase A from porcine pancreas. Biochim. Biophys. Acta 159, 103–117.